



The effect of current rise time on the acceleration of thick flyers to hypervelocities using an electric gun

M.D. Fitzgerald^{a,b,*}, J.D. Pecover^b, N. Petrinic^a, D.E. Eakins^a

^a Department of Engineering Science, University of Oxford, Parks Rd, United Kingdom

^b First Light Fusion, Oxford Industrial Park 10, Meads Rd, United Kingdom

ARTICLE INFO

MSC:
00-01
99-00

Keywords:

Projectile launcher
Electromagnetic acceleration
Electrothermal acceleration
Hypervelocity impact
Magnetohydrodynamics
Pulsed-power
Capacitor bank

ABSTRACT

The electric gun is a projectile launcher which utilises both the rapid expansion of an ohmically heated exploding foil and strong electromagnetic forces to accelerate an insulating flyer up to 20 km/s. The gun's acceleration mechanism is highly efficient at converting stored electrical energy in the pulsed-power device driving the load to kinetic energy in the flyer, with values of up to 25% reported (Osher et al., 1990). This high efficiency would allow capacitor banks to use less energy than conventional drives to generate higher pressure states in materials of interest to extreme state research. Despite its promising efficiency, the electric gun is rarely used, as the process of launching flyers above 0.5 mm thickness in this manner is highly variable, often resulting in uncontrolled launch characteristics and premature failure of the flyer. The gun is also difficult to optimise without use of a sophisticated multi-physics hydrocode, further limiting its take-up. This work presents experimental results from the successful launch of 24×24 mm flyers up to 2.0 mm thick to 10 km/s using an electric gun load on 1.2 MJ pulsed-power device: Machine 3. In combination with results from a 0D model, these findings are used to identify the mechanism for the destruction of thick flyers accelerated using electric guns, including strategies for mitigating their break-up. The results support the existing idea that flyer failure can be avoided by limiting the maximum pressure within the flyer. They also reveal a second mechanism by which the flyer integrity can be maintained when the current rise time is longer than the flight time; high pressures in thick flyers caused their density to remain high enough to prevent the driving foil plasma from breaking through, averting their disassembly. This second mechanism provides a route to accelerate thick electric gun flyers to higher velocities with efficiencies up to around 9% whilst lengthening the shock duration on impact, broadening the gun's potential applications in extreme state research.

1. Introduction

Research into the behaviour of materials at extreme states involves an advancement of scientific knowledge relevant to many of the most consequential challenges faced by humanity today. The pressures and temperatures experienced in aerospace and nuclear fusion applications are, by their nature, found nowhere naturally on the Earth's surface. In order to design and improve hardware for these purposes, the response of materials under the conditions generated during operation must be understood, requiring access to these states in a controlled setting. The electric gun is a pulsed-power device used to access extreme pressure states, through the impact of thin flyers launched up to 20 km/s using the rapid discharge of a capacitor bank. The gun was originally developed at Lawrence Livermore National Laboratory (LLNL) in the 1970s, [1–3], though it has received limited attention in recent years [4–6]. The technique has the advantage of driving highly

planar shocks over a large material volume, simplifying the acquisition of diagnostics [2].

The electric gun can be thought of as a hybrid between an exploding foil initiator (EFI), also known as a ‘slapper’, and an electromagnetic (EM) plate flyer launcher [7,8]. Its projectile is driven by both a thermal explosion, as in an EFI, and the magnetic acceleration of the plate flyer. The process begins with the discharge of a high-speed capacitor bank across a thin metallic foil, resulting in a large amount of energy deposited in the foil through ohmic heating. This energy deposition drives a change of state in the foil from a solid to a rapidly expanding plasma. The ‘exploding’ foil plasma acts as a driver gas, accelerating an adjacent thin insulating plate, referred to as the ‘flyer’. The flyer plate is laid atop the foil in a bonded stiff assembly, such that the foil plasma ‘punches out’ a section of the flyer material, accelerating it typically for a few millimeters to impact a target. This plasma pressure component

* Corresponding author at: Department of Engineering Science, University of Oxford, Parks Rd, United Kingdom.

E-mail address: mila.fitzgerald@outlook.com (M.D. Fitzgerald).

of the acceleration is known as the thermal drive. When large currents are discharged to vaporise the foil, considerable magnetic forces exist in the system that also act to accelerate the foil plasma. This effect is the origin of the magnetic drive. The approach is highly efficient, demonstrating conversion from electrical capacitor bank discharge to projectile kinetic energy of up to 25% [9]. By comparison, EM plate flyers launched on the Z machine at Sandia demonstrate efficiencies closer to 4% [10,11].

The behaviour of the flyer in the electric gun is highly dependent on the characteristics of the capacitor bank powering it, such as current amplitude and rise time. Early investigations into the electric gun sought to optimise its performance by reducing the current rise time of the capacitor bank. This was to ensure the foil explosion occurred near peak current, thereby maximising the thermal energy extracted on launch [12]. However, researchers noted that on high energy capacitor banks the more significant contribution to the flyer acceleration came from the magnetic drive [13]. The resulting short rise time electric gun was found to be successful at launching thin flyers to hypervelocities, but researchers struggled to launch ‘thick’ flyers (over 0.5 mm) without inducing violent state change in the flyer during launch and flight. In high energy electric guns the effect is more extreme; thick flyers often experience complete disintegration shortly after launch [14]. The mechanism by which thick flyers are damaged in short rise time electric guns is not well understood, and researchers at the time lacked the numerical and experimental tools to determine the cause [9]. This stumbling block in the optimisation of electric gun performance prevented the gun from investigating longer timescale phenomena, and the technique fell into disuse due to its limited applications.

Recent developments made to the electric gun have taken advantage of improvements in numerical simulation and diagnostic techniques to begin to address the problems with thick flyer launch to hypervelocity. Wang et al. developed a Lagrangian hydrodynamic code with an equation of state database to more accurately model the foil burst and magnetic acceleration. This enabled them to achieve launch of flyers up to 14 km/s on a short rise time machine, though they did not launch flyers over 0.2 mm thick [5,15]. Conversely, Song et al. focused their efforts on modelling the flyer impact using LS-DYNA [16] and improving their diagnostic technique, leading them to successfully launch a 1.0 mm flyer over a 14 mm flight distance. Song proposed that the flyer’s maintained integrity was a result of their capacitor bank’s long rise time (1.8–2.0 μ s). However, the models used in both investigations did not include the framework to estimate the flyer state and the diagnostics fielded were only used to measure the flyer thickness and velocity. As a result, the mechanisms for both the destruction of thick flyers on the short rise time electric gun and their improved integrity on the long rise time machine remained unclear.

If the mechanisms responsible for the disintegration of thick flyers launched by the electric gun were understood, these destructive states could be anticipated and potentially avoided. This could enable the electric gun to become both an efficient and versatile projectile launcher, making it a powerful complementary tool for existing launch platforms. In this work a numerical model, capable of simulating the electric gun dynamics and flyer pressure state, was used to investigate the difference in the evolution of the state of thick flyers on a short rise time and a long rise time capacitor bank. The results of this study were then used to inform the design of an experimental electric gun load for a 2 μ s rise time, 1.2 MJ pulsed-power device. Finally, a range of diagnostic data collected from these shots, combined with results from the numerical model, was used to answer the following questions:

- What is the dependence of the maximum internal pressures in thick flyers on the machine rise time?
- How does changing the flyer thickness influence flyer state on long rise time electric guns?
- How does the pressure state in the foil and flyer influence electric gun dynamic performance?

Addressing these questions will enable the mechanism responsible for flyer break-up to be determined and importantly should lead to strategies for improving flyer survivability.

2. Numerical modelling: The effect of rise time on flyer state

In this work, data from both a 0-dimensional (0D) model and experimental launch were acquired to build a more comprehensive understanding of the mechanism responsible for the failure of thick flyers launched by the electric gun. *In-situ* collection of data regarding the flyer state during launch and flight prior to impact is challenging, necessitating results obtained through numerical modelling to contribute to the interpretation of the diagnostic data that can be obtained experimentally.

Previous electric gun research has suggested that minimising the current rise time when launching thin flyers leads to an improved performance. However, these load configurations were unable to reliably launch flyers with thickness over 0.5 mm without incurring damage. Song et al. suggested the opposite was true for thick flyers; they found the longer rise time of their capacitor bank was advantageous in maintaining the integrity of the 1 mm thick flyers launched in their experiments. Using a 0D model recently developed by Fitzgerald et al., the acceleration of a square 24.0x24.0x1.5 mm flyer powered by two different pulsed-power machines, Machine 3 (M3) and CEPAGE was simulated [17].

Machine 3 (M3) is a 2.5 MJ pulsed-power machine generally used at First Light Fusion to accelerate EM plate flyers. It is the highest energy capacitor bank used to power an electric gun in open literature, with a long rise time of around 2 μ s. In order to draw comparison, the behaviour of thick flyers was examined both when launched by a long rise time capacitor bank and when accelerated by a short rise time capacitor bank more typical of electric gun launch. CEPAGE is a smaller capacitor bank which has previously been used at First Light Fusion to successfully fire electric gun flyers to over 10 km/s. Further details of both launchers are available in previous works [18–20].

2.1. Method

The electric gun model utilised in this work calculates the dynamics and pressure state of an insulating electric gun flyer in 0D. The model is flexible, with a number of input parameters, including the geometries of the foil and flyer and machine parameters which allow it to calculate results for a wide range of load designs, illustrated in Fig. 1b. The model’s algorithm can be divided into four stages: firstly, the current is calculated at each timestep. This is then used to find state of the foil, and update three positions in the electric gun system: the rear of the foil (z_r), the interface between the foil and flyer (z_i) and the front of the flyer (z_f). Finally, it calculates the pressure at the foil-flyer interface and the maximum pressure in the flyer by using the position of the magnetic field along the z -axis ($z_{p_{max}}$) to find the location of the maximum pressure in the foil. These positions and axes are illustrated in Fig. 2.

In a typical electric gun model, the system dynamics are calculated by adding the foil and flyer mass and determining the system momentum change. The resultant velocities of the foil and flyer are then used to update the foil’s position, which does not account for the time for pressure information to be passed from the foil to the flyer. Whilst this approximation is valid for thin foils and flyers, as the wave transit can be assumed small when compared to the total flight time, the time necessary to communicate a change in velocity in the foil becomes significant when the foil or flyer is thick. This is particularly critical during launch, as the flyer is unable to move off until the first pressure wave has reached its leading surface.

To approximate the 1D delays in communication of pressure information in 0D, the foil and flyer are simplified in space to key locations along the z -axis. The model tracks three positions; the rear of the foil,

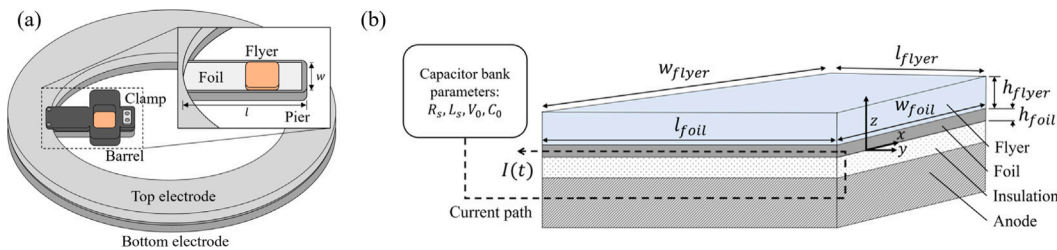


Fig. 1. (a) Simplified diagram showing the electric gun load set-up, with pier foil width (w) and length (l) labelled. The close up shows the flyer atop the foil over the pier, with the barrel hidden from view. The current passes from the pier on the bottom electrode through the foil to the top electrode. (b) The 0D model allows the user to input detailed parameters regarding the foil, flyer and capacitor bank. These include the foil and flyer material and dimensions, and the capacitor bank parameters necessary for calculating the system current at each timestep.

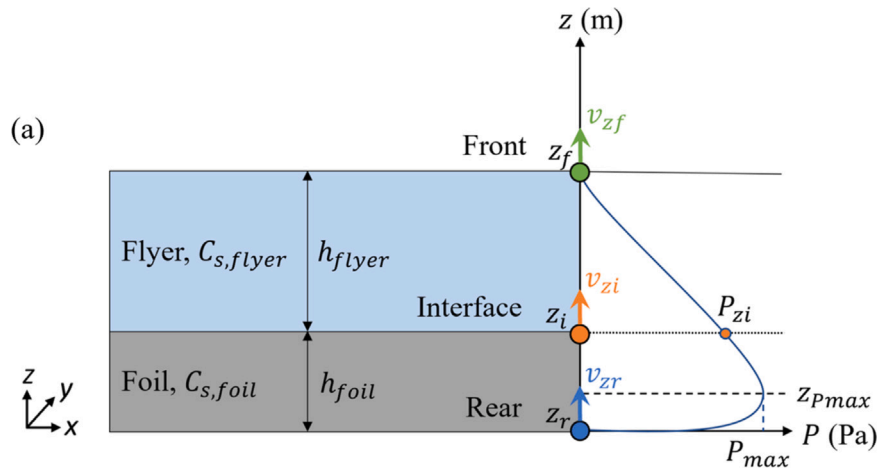


Fig. 2. The positions of the four locations used to determine the pressure at the foil-flyer interface, alongside the velocities used to approximate the foil-flyer dynamics. The model assumes the foil and flyer form a continuous interface, with pressure at the front of the flyer set to zero and the pressure a linear gradient between z_{pmax} and z_f .

the foil-flyer interface and the front of the flyer, visualised in Fig. 2. Prior to launch, the velocity at the rear (v_{zr}) can be found using the total force driving the foil. This velocity state is then assumed to sweep through the foil in the z -direction at the relevant speed of sound, leading to an interface velocity (v_{zi}) found through,

$$v_{zi}(t) = v_{zr} \left(t - \frac{h_{foil}(t)}{c_{s, foil}} \right), \quad (1)$$

where $c_{s,foil}$ is the ambient speed of sound in the foil and $h_{foil}(t)$ is the updated foil thickness. For simplicity, the model assumes the speed of sound to be constant in all materials. As the foil typically accelerates to velocities higher than the flyer sound speed within hundreds of nanoseconds, the interface position can overrun the flyer front if left unchecked. To avoid this, the algorithm instead updates the front velocity using either the speed of sound in the flyer or the interface velocity to approximate shock behaviour that may occur in the flyer using,

$$v_{zf}(t) = \begin{cases} v_{zr} \left(t - \left(\frac{h_{foil}(t)}{c_{s,foil}} + \frac{h_{flyer}(t)}{c_{s,flyer}} \right) \right) & v_{zi}(t) \leq c_{s,flyer} \\ v_{zr} \left(t - \left(\frac{h_{foil}(t)}{c_{s,foil}} + \frac{h_{flyer}(t)}{v_{zi}(t)} \right) \right) & v_{zi}(t) > c_{s,flyer}, \end{cases} \quad (2)$$

where $c_{s, flyer}$ is the speed of sound in the flyer, and $h_{flyer}(t)$ is the updated flyer thickness. The foil and flyer thicknesses are recalculated at the beginning of each timestep using the positions derived from the three location velocities at each timestep. This allows the model to capture the effect of compression and expansion in the foil and flyer despite being OD.

To reduce the computational resource required by the model, the algorithm determines the maximum pressure state in the flyer without

referring to an equation of state. This is done by assuming the pressure state at foil-flyer interface is continuous throughout acceleration and the gradient between the maximum pressure in the foil (P_{max}) and the pressure at the front of the flyer (P_{zf}) is linear. As a result, the gradient of the pressure ($\frac{dP}{dx}$) can be found using,

$$\frac{dP}{dz} = \frac{P_{zf} - P_{max}}{z_i - z_{p_{max}} + h_{f|_{ver}}}. \quad (3)$$

When launch occurs in a vacuum, the model assumes P_f to be zero. Hence the pressure at the interface P_{zi} is simply calculated using,

$$P_{zi} = P_{max} + \frac{dP}{dz}(z_i - z_{P_{max}}). \quad (4)$$

where an example of this gradient is visualised in Fig. 2.

The inclusion of Eqs. (2) and (4) allow the model to capture the changing maximum pressure in the flyer due to the building of thermal pressure in the foil prior to launch and the physical proximity of the position of maximum pressure in the foil to the foil-flyer interface in 0D. The 0D model was verified against 1D simulations in MHD Eulerian hydrocode ‘Code B’, known simply as \mathbb{B} . Fitzgerald et al. found the 0D model most closely matched the 1D MHD simulations for loads with thin foils ($t < 0.5$ mm), as the approximations made to determine $z_{P_{max}}$ and P_{max} became less accurate at late flight times in thick plates [17]. The results for a load on M3 described in Table 2, with $l = 25$ mm, from \mathbb{B} and the 0D model are shown in Fig. 3. The model is able to closely replicate both the magnitude and temporal evolution of the maximum pressure in the flyer and the flyer velocity predicted by \mathbb{B} . This indicates despite the simplifications, the 0D model is able to capture the key physics dominating both the flyer pressure state and dynamics.

The 0D model makes it possible to predict the maximum pressure and flyer velocity, significantly reducing the computational resource

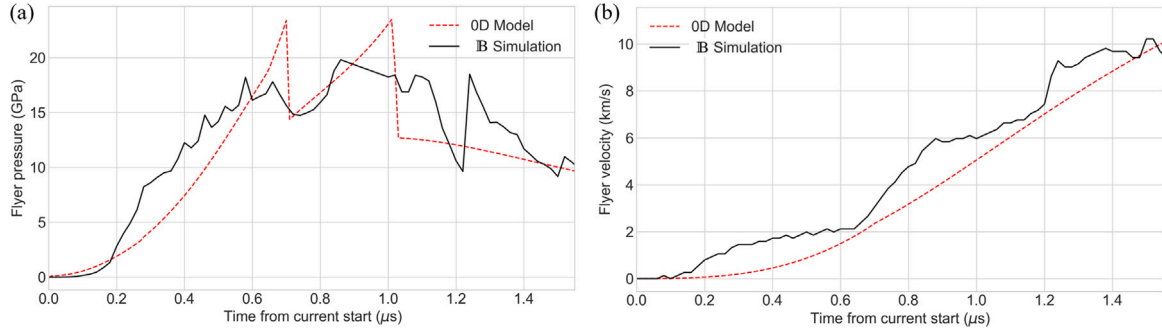


Fig. 3. Comparison between maximum flyer pressure (a) and flyer velocity (b) calculated by the OD model and 1D MHD simulations in \mathbb{B} for a 1.5 mm thick flyer used on M3.

Table 1

Machine parameters for pulsed-power capacitor banks M3 and CEPAGE.

Parameters	M3	CEPAGE	[units]
Charge voltage	140	70	[kV]
Capacitance	124.8	32.0	[μF]
Fixed resistance	0.1	3.0	[μΩ]
Fixed inductance	12.5	5.4	[nH]

Table 2

Electric gun load parameters used in OD simulations.

Load parameters	Value
Foil length	50.0 mm
Foil width	25.0 mm
Foil thickness	0.1 mm
Foil material	Aluminium
Flyer length	25.0 mm
Flyer width	25.0 mm
Flyer thickness	1.5 mm
Flyer material	PMMA

required to investigate the electric gun. The model is used in this investigation to show how the electric gun can be optimised for a specific capacitor bank without the need for a complex multi-physics hydrocode, making the gun a more accessible tool for existing pulsed-power platforms. As the model is able to accept a range of details regarding the load design and machine parameters, the specific response of the flyer to the load design and two capacitor bank can be captured. The machine parameters utilised in this investigation are shown in Table 1 and the load parameters considered by the model are listed in the Table 2.

2.2. Results

The effect of current rise time on the temporal evolution of the flyer pressure was considered by using the OD model to simulate the response of the same electric gun load powered by two different capacitor banks. Fig. 4a shows the time-dependence of the maximum pressure in the flyer within the first 2.5 μs of current start alongside the trajectories of the foil and flyer. An initial peak in the maximum pressure in the flyer can be seen with both machines on launch. This is due to the building of thermal pressure in the exploding foil prior to the launch of the flyer. When the flyer is thin, the time taken to communicate the pressure information from the foil to the front of the flyer is negligible. However, as the flyer thickness increases, the subsequent time elapsed from current start to flyer launch, which in this work is considered to be the time the front of the flyer moves, becomes significant when compared to the current rise time. As a result, by the time the flyer launched by CEPAGE has moved off, the current begins to drop and the pressure in the foil plasma drops. In turn, the maximum flyer pressure also decreases.

By contrast, due to its slow rise time, the maximum pressure in the flyer launched by M3 has multiple maxima. The first, as in the case of CEPAGE, is due to the building thermal pressure in the foil prior to launch. The second is related to the movement of the position of maximum foil pressure within the foil as the magnetic field diffuses through the metal plasma. Fig. 4a demonstrates that the flyer had already travelled 9 mm shortly after the current rise time of around 2.0 μs. M3 not only has a long rise time, but a larger amplitude of around 10 MA, thus the foil remained at an extreme pressure state due to the strong electromagnetic fields in the system until flyer impact. This high pressure in the foil subsequently maintained the pressure at the foil-flyer interface for a greater flight distance. As a result, the maximum pressure in the flyer after the current rise time is still high, with Fig. 4b showing it to be above 15 GPa.

2.3. Discussion

In this section, a comparison is made between the OD modelling results of the electric gun load on the two machines to generate an understanding of how the current rise time of a machine influences the maximum flyer pressure state and the implications this has on flyer integrity. CEPAGE and M3 do not only differ in rise time: the stored energy of M3 is around twice that of CEPAGE. As a result, the magnitude of the current (I) in the exploding foil on M3 is roughly double, impacting the magnitude of the magnetic field strength (B) proportionally and the magnetic pressure (P_B) in the foil by the current squared. As shown in Eq. (5),

$$P_B = \frac{B^2}{2\mu_0} = \frac{(\frac{\mu_0 I}{2w})^2}{2\mu_0}, \quad (5)$$

where w is the foil width, l is the foil length and μ_0 is the vacuum permeability. This relationship is apparent in Fig. 4b, which shows the pressure normalised by the square of the current is similar for both devices. This illustrates that the pressure state in the flyer is strongly dependent on the current through the foil. As a result, the machine rise time will directly influence the evolution of the pressure state in the flyer. After around 1.0 μs, the flyer pressure over the current squared falls on M3 when compared to CEPAGE. This is because as the foil accelerates rapidly to faster than the speed of sound in the flyer, the flyer becomes compressed. When the flyer thickness decreases during flight, the pressure gradient across the foil to the front of the flyer changes relative to the foil-flyer interface. This concept is illustrated in Fig. 5a.

Experimental results have suggested that increasing the machine rise time led to improved flyer integrity in thick flyers [6]. As the maximum pressure state in the flyer is proportional to the square of the current through the foil, when the rise time is long, the pressure in the flyer remains high for a longer period. On the other hand, in short rise time machines the pressure will quickly rise and fall. This suggests that the maintained high pressure in the flyer material at the foil-flyer interface contributes to preventing the flyer from disintegrating during

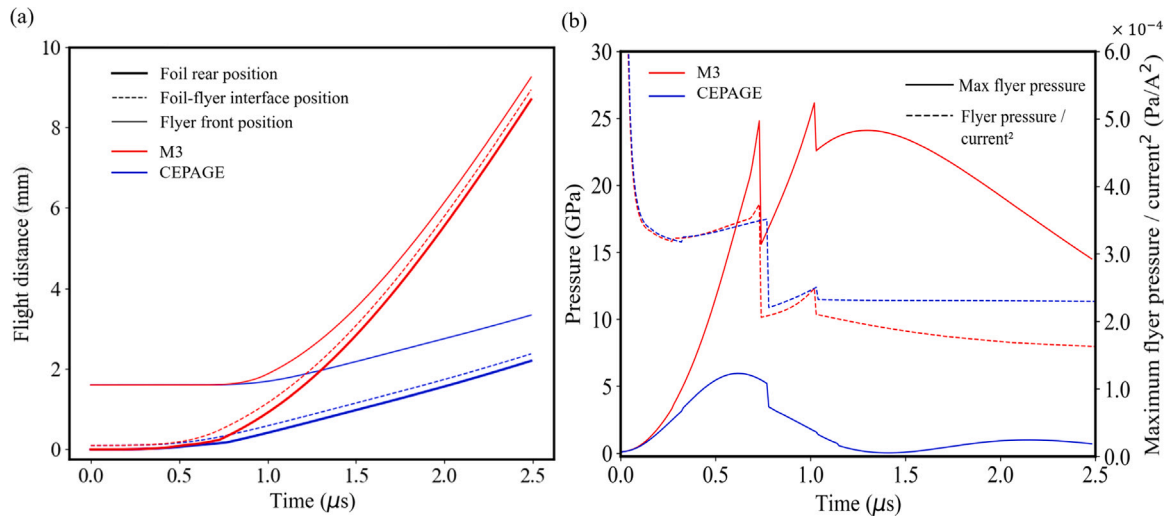


Fig. 4. Plots tracking the temporal evolution of foil-flyer position, maximum pressure (a) and pressure normalised by foil current in the flyer (b) calculated by the OD model throughout launch and flight. M3 has a higher energy and longer current rise time than CEPAGE, therefore the foil and flyer travel further and remain at higher pressures.

flight. It was hypothesised that if the flyer material adjacent to the foil is held at high pressure, the density of the flyer will also be maintained in this region, preventing the exploding foil from breaking through the flyer. In this scenario, it is expected that thicker flyers would be more likely to survive than thin, provided the current pulse length was longer than the flight time to the target. Fig. 5b shows that the OD model predicts the maximum flyer pressure increases with the flyer thickness throughout flight. By the same logic, thick flyers could be destroyed if the current pulse length was shorter than the flight time, as the pressure in the flyer rapidly increases and falls before the flyer had time to impact a target. Fig. 4a shows on CEPAGE, the pressure in the flyer has dropped before the front has moved even 2 mm. If the initial pressure rise was high enough to cause the polymer to lose material strength, as the pressure drops the density could fall below solid state, allowing the foil plasma to break through. The plasma pushing through the flyer would then cause it to break up, resulting in disassembly. This narrative is consistent with the experimental observations made by Osher et al., who noted that their thick flyers broke up almost immediately after moving off [9].

The OD model lacks an equation of state or constitutive model in the flyer material, thus the flyer density and integrity cannot be simulated. Without this information, the prediction that thick flyers keep their integrity on long rise time machines due to their maintained pressure state cannot be verified. To investigate the effect of the flyer pressure on the flyer density state and dynamics discussed in this section further, experimental testing of the electric gun load on M3 was performed. The diagnostics data collected was then used in parallel with the OD modelling results to build a more complete picture of the relationships between flyer thickness, flyer state, rise time and load efficiency.

3. Experimental testing: parametric study of flyer thickness on a 1.2 MJ electric gun

In this section the experimental method and data from electric gun shots on M3 using the load design investigated in the OD model are presented. The results in the previous section suggest that the disintegration of thick flyers on short rise time machines and the maintained integrity of thick flyers on long rise time machines are a result of maintained high pressures in the flyer material adjacent to the foil-flyer interface. However, owing to its simplicity, the OD model is unable to model several mechanisms which could contribute to the loss of the flyer's integrity. These include, but are not limited to, material strength, compressibility and circuit discharge effects.

Flyer thicknesses from 0.25 mm to 2.0 mm were launched over 9.0 mm flight distance, and a 0.5 mm flyer was launched over 20.0 mm distance. A more complete picture of the effect of flyer thickness on flyer state using long rise time electric guns was determined by evaluating the velocity of these flyers, measuring their shock velocities imparted on impact in a target and mapping their leading surface during flight.

3.1. Method

The experimental set up used in this work is shown in Fig. 6a, which illustrates the foil, flyer and barrel in relation to the diagnostics fielded on the shots. Measurements of the flyer state and velocity are required to characterise the operation of the gun. This necessitates acquiring the flyer's impact speed and the shock speed in a known material. The velocity profile of the flyer provides key additional data to build a more detailed picture of the processes at play. The shock speed in a target is found by projecting a 1D line of laser light through a transparent PMMA target block. As the flyer impacts the block, it induces a shockwave of a high enough pressure (over 20 GPa) to turn the PMMA opaque, thus blocking the laser light. The 1D laser is captured by a streak camera, and the position of the shock front through the block is tracked through time. 1D and 2D VISAR are fielded on the flyer, measuring the velocity of the flyer throughout flight and mapping its damage features respectively. Finally, a high speed camera images the target block in 2D to capture the shock shape and evaluate the flyer planarity and integrity on impact.

Attempting to collect diagnostic data from flyers launched to hypervelocity on the electric gun is challenging. This is especially true for thick flyers, as the launch process often results in the abrupt disruption of the flyer's leading surface. This can result in the reduction of surface reflectivity, preventing the collection of 1D VISAR. If the surface disruption is a result of foil plasma breaking through the flyer, the bright, high velocity plasma will overtake the flyer obscuring the 1D and 2D VISAR line of sight and causing a low speed precursor shock in the target block. Finally, large volumes of foil plasma escaping from below the top electrode fill the space around the barrel on burst. Without protective measures, this plasma can escape into the mirror mount, obscuring the flyer impact event.

Adaptations to the experimental set up to improve diagnostic acquisition are shown in Fig. 6b. For example the PMMA target block was tilted to eliminate ghost fringes caused by reflection of the VISAR laser at the block faces, such that laser light reflected by the flyer was more apparent. Secondly, the flyer was fixed into a recess at the bottom of

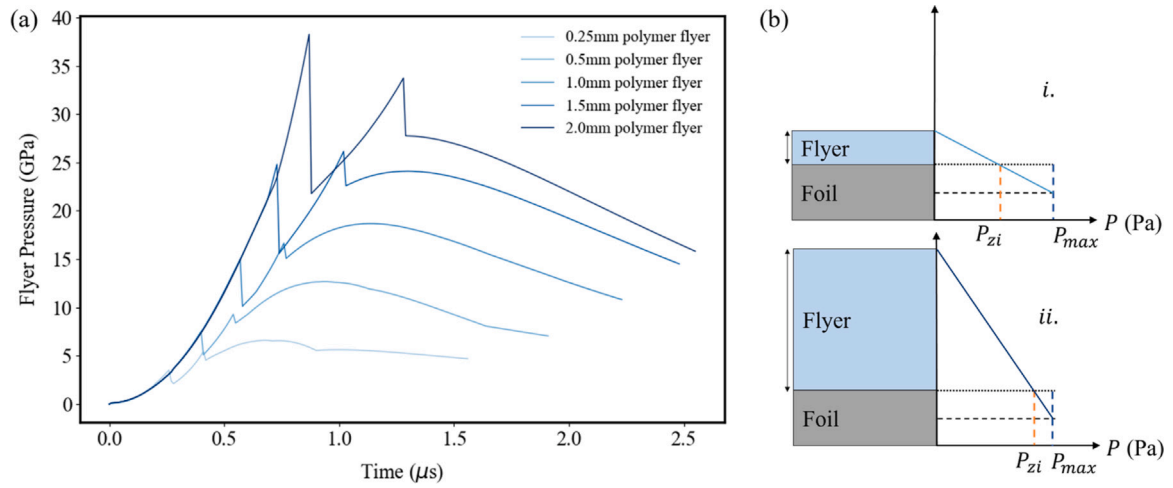


Fig. 5. (a) Qualitative illustration of the mechanism for the higher pressures in thicker flyers later in flight. As the position of the front of the flyer is further away from maximum pressure in *ii* relative to the position of the foil-flyer interface, the maximum pressure in the flyer is greater. (b) Plot showing the temporal evolution of the maximum flyer pressure in flyers of different thicknesses launched by M3 over a flight distance of 9 mm. The initial spike in pressure increases with flyer thickness as the launch time occurs later. The pressure remains higher in thick flyers later due to the orientation of the pressure gradient between the pressure maximum in the foil and the flyer front, illustrated in Fig. 5a.

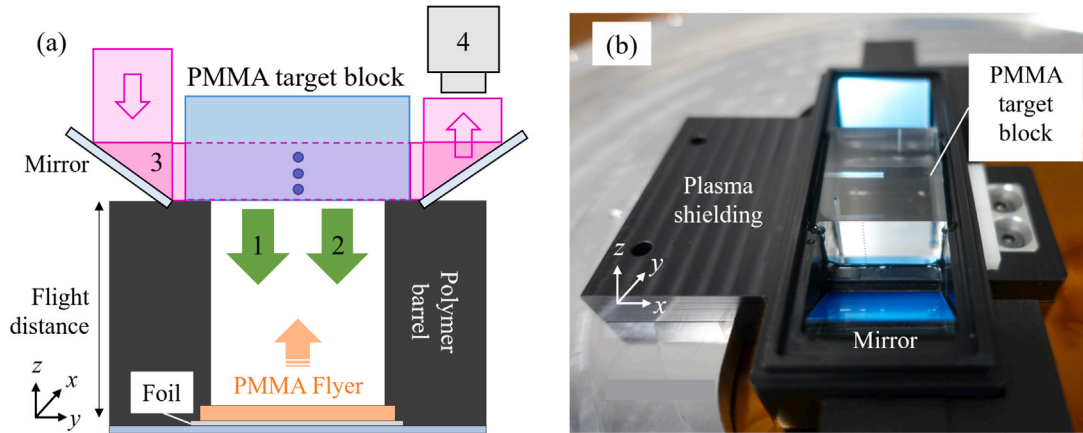


Fig. 6. (a) Diagnostics fielded during the experiment include (1) 1D VISAR streak measuring projectile velocity, (2) 2D VISAR fringes mapping flyer surface damage evolution during flight, (3) 1D laser streak capturing shock velocity profile in the target block and (4) high speed imaging of the PMMA target block showing the shock front in 2D. (b) Image of barrel with plasma shielding, target block and mirror mount.

Table 3

Electric gun shot results using load seen in Fig. 1a, 0.1 × 25 × 50 mm Al foil, 24 × 24 mm polyimide flyer. Shots 1 and 3 failed midflight due to plasma breakthrough.

Shot no.	Flyer thickness (mm)	Flight distance (mm)	Maximum shock speed in target (km/s)	Flyer survived until impact?
1	0.25	9.0	7.0	No
2	0.5	9.0	8.0	Yes
3	0.5	20.0	8.1	No
4	1.0	9.0	9.55	Yes
5	1.5	9.0	9.8	Yes
6	2.0	10.0	10.6	Yes

the barrel to prevent foil plasma from escaping around the edges into the barrel on launch. Lastly, a wall of plastic was integrated into the barrel design over the join between the foil and top electrode, referred to in Fig. 6b as the 'plasma shielding', to protect the line of sight of the mirrors at the top of the barrel.

3.2. Results

The shock speeds in the PMMA target block were successfully obtained for all shots performed. The process for determining the shock speed in the block is illustrated in Fig. 7. The position of shock front

profile was identified and a fifth order polynomial fit was applied to the position data. The fitted data was then differentiated to find the shock speed. For shots 4, 5 and 6 in Table 3, images of the shock front position in the high speed camera are used instead. Again, a fifth order polynomial fit was applied to the shock position data, and the differential of the position data determined the shock velocity in the target. The second technique gave a lower time resolution, but tracked the shock front further through the block and was less sensitive to distortion due to debris in the mirror mount.

Table 3 shows the highest shock speed was generated on impact by the 2.0 mm flyer. The shock speed generated on impact by 2.0 mm flyer of 10.6 km/s in the PMMA target block is equivalent to 70 GPa

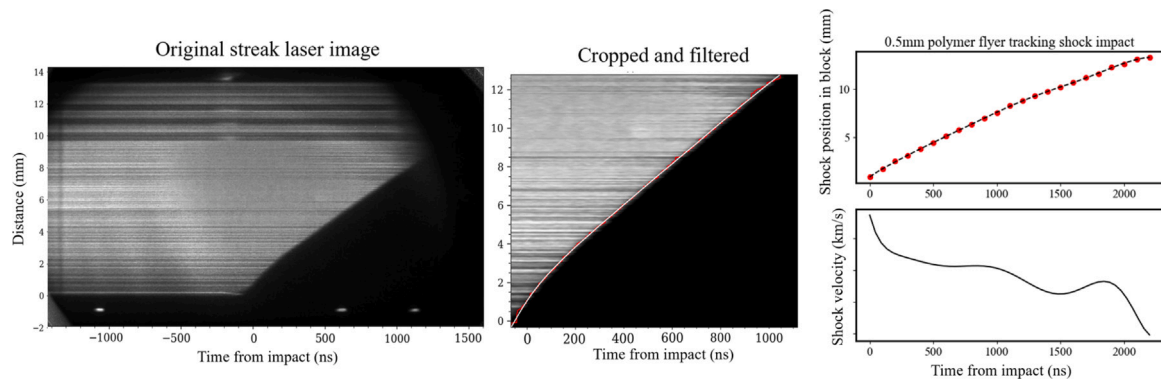


Fig. 7. The velocity of the shock in the transparent PMMA target block is calculated by differentiating the progression of the shock front position in time. First, the position of the shock front is identified: as the shock front moves through the target its high pressure state turns the PMMA opaque, gradually blocking the laser light as it moves. The boundary between the laser light and opaque (black) region for each timestep is identified automatically by evaluating the pixel value, and the positions are extracted. A polynomial fit is then applied to the shock positions which, when differentiated, gives a less noisy shock velocity profile.

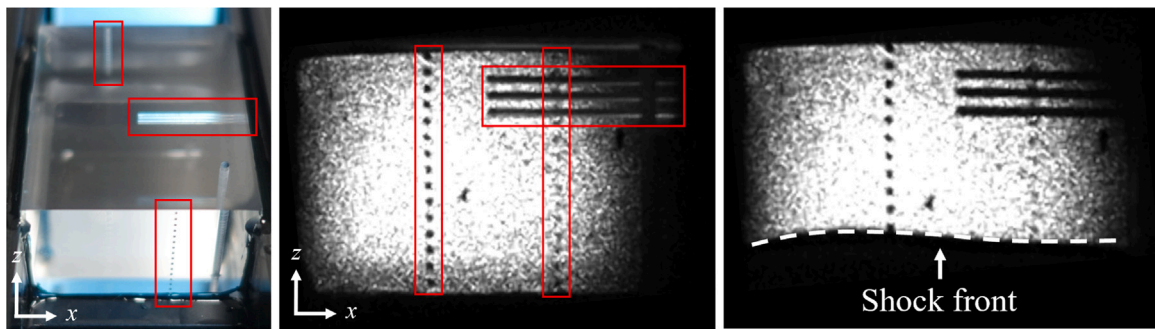


Fig. 8. Images taken using the high speed camera focused on the target block showing an example of the shock front generated on impact using the 1 mm thick flyer (red boxes around fiducial marks relate set up to high speed camera images). The small tilt in the shock front, consistent across all shots performed, could be associated with slight asymmetries in the magnetic field strength across the bottom electrode pier [18].

pressure over a 24x24 mm area [21]. The flat progression of the shock front in the target block, shown in Fig. 8, suggest the thickest flyers retained good planarity and a homogeneous state across their width.

Converse to behaviour expected on a short rise time machine, the diagnostic data for the two thinnest flyers suggest they experienced some disassembly during flight. Fig. 9a shows the initial shock speed in the target is low for both the 0.25 mm flyer at 9 mm barrel length and the 0.5 mm at 20 mm barrel length due to the breakthrough of a low density plasma precursor shock at late times in flight. Fig. 9b shows this process occurring in the 2D VISAR imaging. The bright foil plasma can be seen breaking through the centre of the foil, as opposed to escaping around the edges.

3.3. Discussion: Measured and simulated results

The experimental results collected from the shots performed on M3 demonstrate that the electric gun load designed for this work can accelerate flyers of unprecedented thickness whilst maintaining their integrity until impact. Contrary to previous research performed on short rise time capacitor banks, it was the thinner flyers that experienced disassembly. This loss of integrity in the thin flyers occurred late in the flight time, as opposed to near launch as reported in thick flyers on short rise time electric guns. At the conclusion of the modelling performed in Section 2, it was suggested that the maintained pressure state in thick flyers launched using M3 could contribute to maintaining their integrity. These results support this claim, as the only two flyers which experienced plasma breakthrough had the lowest maximum pressure, demonstrated in Fig. 10a. The 0.25 mm flyer had low maximum flyer pressure due to the lower thermal pressures and reduced pressure gradient, whereas the 0.5 mm flyer launched over

20 mm flight distance experienced a pressure reduction late in the current rise time.

The final impact speed of the flyers at the target was not recorded due to loss of the VISAR signal from the front surface of the flyer around halfway through flight. Without the impact speed, the density of the flyer following impact cannot be estimated. However, comparison between the measured velocity profiles of the measured and simulated velocity profiles, shown in Fig. 10b suggest that, at early times in flight, the OD model is able to predict the experimental velocities with reasonable accuracy. Table 4 shows the final impact times predicted by the OD model approximately match the experimental results, thus the numerically predicted impact speeds are used in this work to estimate the flyer density on arrival in lieu of experimentally recorded velocities. The interfacial continuity conditions state that

$$\rho_f U_f (V_0 - u_f) = \rho_t U_t u_t, \quad (6)$$

where the subscripts f and t denote the flyer and PMMA target block, ρ is density, U is the shock speed, V_0 is the flyer impact velocity and u is the particle velocity. The average density of the flyer can be estimated by combining this equation with the LASL Hugoniot data for polyimide and PMMA [21],

$$U_f = 2.327 \text{ km/s} + 1.34u_f \quad (7a)$$

$$U_t = 2.6 \text{ km/s} + 1.52u_t. \quad (7b)$$

Using the data collected, the calculated flyer densities are shown in Table 5. The results show the density in the flyers on impact increased with their thickness. This trend persists when taking into account the maximum error in the predicted velocity, corresponding to the percentage error in the predicted arrival times shown in Table 4.

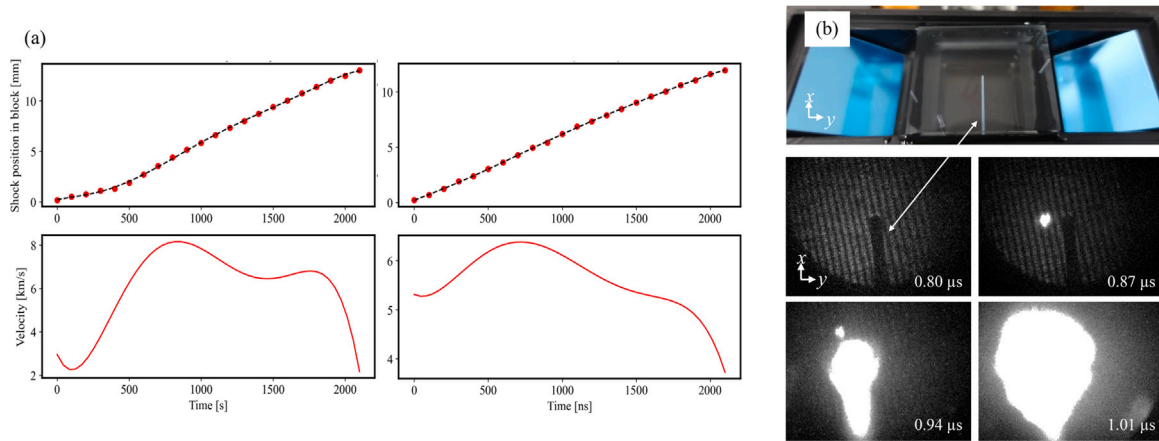


Fig. 9. (a) Plots of the temporal evolution shock in block velocity profiles for the 0.25 mm thick flyer and the 0.5 mm flyer launched over 20 mm. The low initial velocity of the shock in the block in both cases is an indication that a high velocity but low density shock front arrived in the target ahead of the flyer, which on secondary impact caused the later velocity increase. This indicates that foil plasma was able to escape in front of the flyer, suggesting that the flyer experienced a loss of integrity during flight. (b) Images of plasma breaking through the 0.25 mm thick flyer from the 2D VISAR fringes used to map the flyer surface. Its view was oriented down the barrel and the dark shadow of the fiducial marker in the target block can be used for reference. The plasma can be seen to first appear at 0.87 μ s near the centre of the flyer, indicating the plasma forced its way through the flyer instead of escaping around the edges.

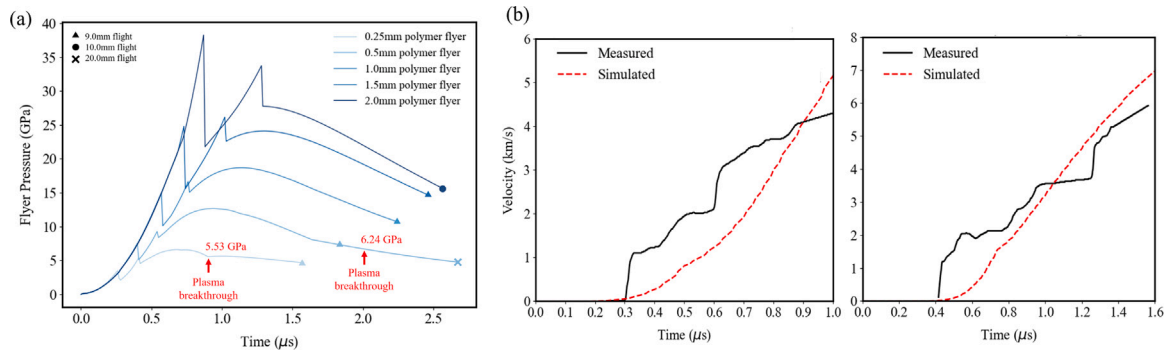


Fig. 10. (a) Plot showing the maximum pressure of the flyers over time launched by M3 calculated by the OD, for the different flyer thicknesses and barrel lengths shot experimentally on M3. The time the 0.25 mm thick flyer and 0.5 mm thick flyer shot to a flight distance of 20 mm experienced plasma breakthrough occurred when the OD model predicted they were at similar pressures. This suggests that the foil plasma was able to force its way through the flyer when the maximum pressure in the flyer material dropped below a certain threshold. (b) The measured 1D VISAR velocity profiles in the early stages of launch and flight for the 0.5 mm and 1.0 mm thick flyers. The OD model has no equation of state in the flyer, so is unable to model the release of the front surface of the flyer into vacuum. However, the simulated velocity is close to the measured profile in both cases, and is likely more indicative of the velocity of densified bulk of the flyer. The impact velocities of the flyers were not captured in this work. However, these results alongside the similar flyer impact times (Table 5) indicate that the impact velocities calculated by the OD can be used instead.

Table 4

Comparison between experimentally measured and modelled impact time.

Shot no.	Measured impact time (μ s)	Predicted impact time (μ s)
2	2.09	1.98
4	2.27	2.13
5	2.21	2.20
6	2.61	2.45

The magnitude of the flyer density corresponds to the predicted maximum flyer pressure predicted by the OD model. Fig. 10a shows the thicker the flyer, the higher the maximum flyer pressure on impact. Similarly, the experimental results find the density of the flyer on arrival increases with flyer thickness. This provides evidence for a more definitive mechanism for maintaining thick flyer integrity on long rise time machines. The thicker the flyer, the higher the maximum flyer pressure throughout flight and the higher the density of the flyer. If the flyer remains dense throughout flight, the foil plasma accelerating it cannot break through the flyer and the flyer maintains its planarity and form.

Finally, the efficiency of the electric gun was approximated by calculating the kinetic energy delivered to the target divided by the machine discharge energy, based on both the flyer and foil mass and

impact speed. The maximum efficiency predicted for this electric gun load was 8.63% in the 2 mm thick flyer. This is below the 25% reported by Osher et al., but remains high for a projectile launcher. For comparison, an aluminium plate flyer of the same mass and surface area as the 2 mm thick polyimide electric gun flyer would have a thickness of around 1.05 mm. For this load geometry, the OD model predicts that the impact speed of the aluminium plate flyer would be 5.1 km/s, which is equivalent to an efficiency of only 1.8 %. This result suggests the electric gun can deliver more energy to a target than an EM plate for the same machine and load design, due to additional thermal pressures in the exploding foil accelerating the insulating flyer.

Table 5 shows the efficiency of the load improved as the flyer thickness increased. This result is likely to be an artifact of M3's long rise time. Thick flyers take longer to launch, thus more energy is deposited in the exploding foil due to the strong electromagnetic forces in the system. As a result, the impact velocity of the 2.0 mm thick flyer is predicted to be higher than the 0.5 mm despite its greater mass. However, the efficiency in the 1.5 mm thick flyer is higher than the 1.0 mm thick flyer, despite having an earlier measured impact time. This suggests that the expansive thermal pressure provides additional acceleration to the flyer. Analysis in Section 2.3 and previous work suggests the thermal pressure in the exploding foil builds prior to

Table 5

The values of flyer impact density calculated using the maximum shock speeds recorded in Table 3 and Eq. (6). Efficiency is considered to be the combined kinetic energy of the foil and flyer divided by the machine energy.

Flyer thickness (mm)	Predicted impact speed (km/s)	Flyer impact density (kg/m ³)	Efficiency %
0.5	10.5	411.0	2.59
1.0	10.05	964.8	4.10
1.5	10.1	1064	5.88
2.0	10.75	1229	8.63

launch, as the electromagnetic pressure rapidly increases whilst the foil volume remains confined [17]. As the time before launch increases with flyer thickness, the thermal pressure becomes greater, contributing greater expansive acceleration forces and therefore improving the load efficiency.

4. Conclusions

In this work, the relationship between flyer integrity and the current rise time in flyers launched using an electric gun load was explored to determine the mechanism behind previously researched damage to thick flyers. Firstly, a simplified OD numerical model was used to simulate the dynamics and maximum flyer pressure of a 1.5 mm thick flyer, launched using identical electric gun loads on two pulsed-power devices with different rise times. The temporal evolution of the maximum flyer pressure using the short rise capacitor bank CEPAGE was found to rapidly increase, before dropping significantly after the current rise time. The time taken to launch thick flyers was longer, due to its higher inertia and delays in communication of the pressure waves. As a result, the pressure in the flyer dropped shortly after launch. On the other hand, the thick flyer launched using the long rise time pulsed-power device M3 was found to maintain high pressures in the flyer until impact. After comparing the two cases, it was proposed that the maintained pressure in the thick flyers on long rise time devices was beneficial in preventing the flyer from breaking up.

To investigate the hypothesis that the extreme pressure state in flyers on long rise time devices contributed to their successful launch, a series of electric gun shots were performed on M3. The data collected from these shots, in combination with impact speeds predicted by the OD model suggested the high pressures in the thick flyers contributed to maintaining a high density region at the foil-flyer interface. Referring to the questions initially posed in the introduction, it was concluded:

- The maximum pressure in the flyer is related to the magnitude of the current, therefore, on long rise time machines higher pressures are maintained in the flyer. The pressure in the flyer throughout flight increases with flyer thickness, due to the flyer's constant contact with the high electromagnetic pressure foil driving it.
- Experimental results from electric gun shots on M3 found that thicker flyers had higher density on impact. Thin flyers with lower pressures were found to experience plasma breakthrough and disassembly at late times.
- The dynamic performance of the electric gun was found to improve as the pressures in the foil and flyer increased. Firstly, the thicker flyers were found to have higher density on impact, which led to higher pressures in the target block. Secondly, the experimentally measured efficiencies were found to improve with flyer thickness, due to the greater thermal pressure developed in foils confined beneath thicker flyers. The maximum measured efficiency of 8.6% was over four times greater than an equivalent EM plate flyer.

Through addressing these questions, the mechanism for thick flyer break-up and strategies to improve flyer survivability were determined. Thick flyers are destroyed on the electric gun when their density drops below a certain value, allowing the high pressure foil plasma driving the flyer to break the flyer apart. If the initial pressure rise

is sufficient, the flyer will lose its material strength properties. As a result, when the pressure in the flyer subsequently drops so does the flyer density. This causes the flyer's disintegration as it mixes with the accelerating exploding plasma behind it. Flyer destruction can therefore be avoided by either taking care to ensure that the flyer does not reach pressures which cause loss of strength, or conversely, by ensuring the pressures in the flyer remains sufficiently high so as to maintain the flyer density throughout flight. This generalised understanding of the flyer destruction mechanisms allows the OD model utilised in this work to design and optimise the electric gun for an arbitrary current pulse shape.

CRedit authorship contribution statement

M.D. Fitzgerald: Conceptualization, Data curation, Formal analysis, Investigation, Methodology, Visualization, Writing – original draft, Writing – review & editing. **J.D. Pecover:** Conceptualization, Methodology, Project administration, Supervision, Writing – review & editing. **N. Petrinic:** Supervision, Writing – review & editing. **D.E. Eakins:** Conceptualization, Methodology, Project administration, Supervision, Writing – review & editing.

Declaration of competing interest

The authors declare that they have no known competing financial interests or personal relationships that could have appeared to influence the work reported in this paper.

Data availability

Data will be made available on request.

Acknowledgements

The authors gratefully acknowledge the support provided by First Light Fusion, both in terms of sponsorship of M. D. Fitzgerald's DPhil, and through skills and expertise of the pulsed power, experimental and numerical teams. Additional thanks to E. Escauriza, R. Barker, J. Read, H. Doyle, C. Dobranski, L. Caballero Bendixsen, P. Holligan, A. Turnball, M. Sasi, G. Jones and J. Darling for their experimental support.

References

- [1] Weingart R, Lee R, Jackson R, Parker N. Acceleration of thin flyers by exploding metal foils: application to initiation studies. [PETN, TATB, PBX-7404, NM]. Tech. rep, California Univ., Livermore (USA). Lawrence Livermore Lab.; 1976.
- [2] Weingart R, Chau H, Goosman D, Hofer W, Honodel C, Lee R, et al. Electric gun: a new tool for ultrahigh-pressure research. Tech. rep, California Univ., Livermore (USA). Lawrence Livermore Lab.; 1979.
- [3] Osher J, Chau H, Gathers G, Lee R, Weingart R. Application of a 100-kV electric gun for hypervelocity impact studies. Int J Impact Eng 1987;5(1–4):501–7.
- [4] Guiji W, Xiangyang D, Fuli T, Jun L, Ning Z, Yan G, et al. Speed test of small size flyer of explosive foil detonator [Ph.D. thesis], Explosion and shock; 2008.
- [5] Wang G, He J, Zhao J, Tan F, Sun C, Mo J, et al. The techniques of metallic foil electrically exploding driving hypervelocity flyers to more than 10 km/s for shock wave physics experiments. Rev Sci Instrum 2011;82(9):095105.
- [6] Song Z, Mo J, Zhao J, Tan F, Yuan H. Study on launching technique of a 98 kJ electric gun for hypervelocity impact experiments. Int J Impact Eng 2018;122:419–30.

- [7] Varesh R. Electric detonators: EBW and EFL. *Propell Explos Pyrotechn* 1996;21(3):150–4.
- [8] Lemke R, Knudson M, Hall C, Hail T, Desjarlais P, Asay J, et al. Characterization of magnetically accelerated flyer plates. *Phys Plasmas* 2003;10(4):1092–9.
- [9] Osher J, Gathers R, Chau H, Lee R, Pomykal G, Weingart R. Hypervelocity acceleration and impact experiments with the LLNL electric guns. *Int J Impact Eng* 1990;10(1–4):439–52.
- [10] Lemke RW, Knudson MD, Davis J-P. Magnetically driven hyper-velocity launch capability at the sandia z accelerator. *Int J Impact Eng* 2011;38(6):480–5.
- [11] Sinars D, Sweeney M, Alexander C, Ampleford D, Ao T, Apruzese J, et al. Review of pulsed power-driven high energy density physics research on Z at sandia. *Phys Plasmas* 2020;27(7).
- [12] Chau H, Dittbenner G, Hofer W, Honodel C, Steinberg D, Stroud J, et al. Electric gun: a versatile tool for high-pressure shock-wave research. *Rev Sci Instrum* 1980;51(12):1676–81.
- [13] Osher JE, Barnes G, Chau HH, Lee RS, Lee C, Speer R, Weingart RC. Operating characteristics and modeling of the LLNL 100-kV electric gun. *IEEE Trans Plasma Sci* 1989;17(3):392–402.
- [14] Lee R, Osher J, Chau H, Pomykal G, Speer R. 1 MJ electric gun facility at LLNL. *IEEE Trans Magnet* 1993;29(1):457–60.
- [15] Wang G, Zhao J, Luo B, Jiang J. Magnetohydrodynamics of metallic foil electrical explosion and magnetically driven quasi-isentropic compression. *InTech*; 2011.
- [16] Hallquist JO, Manual L-DT. Livermore software technology corporation. Livermore, Ca; 1998, 94550–1740.
- [17] Fitzgerald MD, Pecover JD, Petrinic N, Eakins DE. A 0-D electric gun model for the optimization of flyer acceleration to hypervelocities. *IEEE Trans Plasma Sci* 2023.
- [18] Holligan P, Caballero Bendixsen L, Clayson T, Parkin J, Darling J, Bland S, et al. An overview of the diagnostic developments for M3, a 2.5 MJ low inductance capacitor discharge machine. In: APS division of plasma physics meeting abstracts, vol. 2018. 2018, p. GP11–088.
- [19] Fitzgerald M, Eakins D, Pecover J. The design and testing of a novel electric gun: A pulsed power hypervelocity flyer launcher. In: AIP conference proceedings, vol. 2844, no. 1. AIP Publishing; 2023.
- [20] Lefrancois A, Chanal P-Y, Le Blanc G, Petit J, Avrillaud G, Delchambre M. High-velocity flyer-plate developments on two high-pulsed-power generators based on a strip-line design (GEPI and CEPAGE). *IEEE Trans Plasma Sci* 2010;39(1):288–93.
- [21] Marsh SP. LASL shock hgoniot data, vol. 5. Univ of California Press; 1980.